

TNI	Kozmická technika Príručka pre tepelnotechnický návrh Časť 10: Kondenzátor s fázovou premenou	TNI CEN/CLC/TR 17603-31-10 31 0540
------------	--	--

Space engineering - Thermal design handbook - Part 10: Phase - Change Capacitor

Táto technická normalizačná informácia obsahuje anglickú verziu CEN/CLC/TR 17603-31-10:2021.
This Technical standard information includes the English version of CEN/CLC/TR 17603-31-10:2021.

Táto technická normalizačná informácia bola oznámená vo Vestníku ÚNMS SR č. 12/21

TECHNICAL REPORT
RAPPORT TECHNIQUE
TECHNISCHER BERICHT

**CEN/CLC/TR 17603-31-
10**

August 2021

ICS 49.140

English version

**Space engineering - Thermal design handbook - Part 10:
Phase - Change Capacitor**

Ingénierie spatiale - Manuel de conception thermique -
Partie 10 : Réservoirs de matériaux à changement de
phase

Raumfahrttechnik - Handbuch für thermisches Design -
Teil 10: Kondensatoren mit Phasenübergängen

This Technical Report was approved by CEN on 21 June 2021. It has been drawn up by the Technical Committee CEN/CLC/JTC 5.

CEN and CENELEC members are the national standards bodies and national electrotechnical committees of Austria, Belgium, Bulgaria, Croatia, Cyprus, Czech Republic, Denmark, Estonia, Finland, France, Germany, Greece, Hungary, Iceland, Ireland, Italy, Latvia, Lithuania, Luxembourg, Malta, Netherlands, Norway, Poland, Portugal, Republic of North Macedonia, Romania, Serbia, Slovakia, Slovenia, Spain, Sweden, Switzerland, Turkey and United Kingdom.



**CEN-CENELEC Management Centre:
Rue de la Science 23, B-1040 Brussels**

Table of contents

European Foreword.....	8
1 Scope.....	9
2 References	10
3 Terms, definitions and symbols	11
3.1 Terms and definitions	11
3.2 Abbreviated terms.....	11
3.3 Symbols.....	12
4 Introduction.....	14
5 PC working materials	15
5.1 General.....	15
5.1.1 Supercooling	15
5.1.2 Nucleation	19
5.1.3 The effect of gravity on melting and freezing of the pcm	20
5.1.4 Bubble formation	21
5.2 Possible candidates.....	21
5.3 Selected candidates	28
6 PCM technology	52
6.1 Containers	52
6.2 Fillers.....	52
6.3 Containers and fillers	53
6.3.1 Materials and corrosion.....	53
6.3.2 Existing containers and fillers	56
7 PCM performances	60
7.1 Analytical predictions	60
7.1.1 Introduction	60
7.1.2 Heat transfer relations.....	61
8 Existing systems	67
8.1 Introduction.....	67

CEN/CLC/TR 17603-31-10:2021 (E)

8.2	Dornier system	68
8.3	Ike	81
8.4	B&k engineering	101
8.5	Aerojet electrosystems	106
8.6	Trans temp	116
Bibliography.....		126

Figures

Figure 5-1: Temperature, T , vs. time, t , curves for heating and cooling of several PCMs. From DORNIER SYSTEM (1971) [9].....	18
Figure 5-2: Temperature, T , vs. time, t , curves for heating and cooling of several PCMs. From DORNIER SYSTEM (1971) [9].....	19
Figure 5-3: Density, ρ , vs. temperature T , for several PCMs. From DORNIER System (1971) [9].....	47
Figure 5-4: Specific heat, c , vs. temperature T , for several PCMs. From DORNIER System (1971) [9].....	48
Figure 5-5: Thermal conductivity, k , vs. temperature T , for several PCMs. From DORNIER System (1971) [9].....	49
Figure 5-6: Vapor pressure, p_v , vs. temperature T , for several PCMs. From DORNIER System (1971) [9].....	50
Figure 5-7: Viscosity, μ , vs. temperature T , for several PCMs. From DORNIER System (1971) [9].....	51
Figure 5-8: Isothermal compressibility, χ , vs. temperature T , for several PCMs. From DORNIER System (1971) [9].....	51
Figure 6-1: Container with machined wall profile and welded top and bottom. Honeycomb filler with heat conduction fins. All the dimensions are in mm. From DORNIER SYSTEM (1972) [10].....	57
Figure 6-2: Fully machined container with welded top. Honeycomb filler. All the dimensions are in mm. From DORNIER SYSTEM (1972) [10].	58
Figure 6-3: Machined wall container profile with top and bottom adhesive bonded. Alternative filler types are honeycomb or honeycomb plus fins. All the dimensions are in mm. From DORNIER SYSTEM (1972) [10].	59
Figure 7-1: Sketch of the PCM package showing the solid-liquid interface.	61
Figure 7-2: PCM mass, M_{PCM} , filler mass, M_F , package thickness, L , temperature excursion, ΔT , and total conductivity, k_T , as functions of the ratio of filler area to total area, A_F/A_T . Calculated by the compiler.	65
Figure 7-3: PCM mass, M_{PCM} , filler mass, M_F , package thickness, L , temperature excursion, ΔT , and total conductivity, k_T , as functions of the ratio of filler area to total area, A_F/A_T . Calculated by the compiler.	66
Figure 8-1: PCM capacitor for eclipse temperature control developed by Dornier System.	71
Figure 8-2: 30 W.h PCM capacitors developed by Dornier System. a) Complete PCM capacitor. b) Container and honeycomb filler with cells normal to the heat	














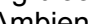
CEN/CLC/TR 17603-31-10:2021 (E)

input/output face. c) Container, honeycomb filler with cells parallel to the heat input/output face, and cover sheets.....	71
Figure 8-3: PCM mounting panels developed by Dornier Syatem. b) Shows the arrangement used for thermal control of four different heat sources.....	72
Figure 8-4: Thermal control system formed by, from right to left, a: PCM capacitor, b: axial heat pipe and, c: flat plate heat pipe. This system was developed by Dornier System for the GfW-Heat Pipe Experiment. October 1974.....	76
Figure 8-5: PCM capacitor shown in the above figure.....	76
Figure 8-6: Temperature, T , as selected points in the complete system vs. time, t , during heat up. a) Ground tests. Symmetry axis in horizontal position. $Q = 28$ W. b) Ground tests. Symmetry axis in vertical position. $Q = 28$ W. The high temperatures which appear at start-up are due to pool boiling in the evaporator of the axial heat pipe. c) Flight experiment under microgravity conditions. Q not given. notice time scale.....	77
Figure 8-7: PCM capacitor developed by Dornier System for temperature control of two rate gyros onboard the Sounding Rocket ESRO "S-93".	79
Figure 8-8: Test model of the above PCM capacitor. In the figure are shown, from right to left, the two rate gyros, the filler and the container.....	79
Figure 8-9: Temperature, T , at the surface of the rate gyros, vs. time, t . — Ambient temperature, $T_R = 273$ K. — Ambient temperature, $T_R = 273$ K. — — Ambient temperature changing between 273 K and 333 K. — — This curve shows the history of the ambient temperature used as input for the last curve above. References: DORNIER SYSTEM (1972) [10], Striimatter (1972) [22].....	80
Figure 8-10: Location of the thermocouples in the input/output face. The thermocouples placed on the opposite face do not appear in the figure since they are projected in the same positions as those in the input/output face. All the dimensions are in mm.	83
Figure 8-11: Prototype PCM capacitor developed by IKE. All the dimensions are in mm. a: Box. b: Honeycomb half layer. c: Perforations in compartment walls. d: pinch tube. e: Extension of the pinch tube.	85
Figure 8-12: Time, t , for nominal heat storage and temperature, T of the heat transfer face vs. heat input rate, Q . ○ Time for nominal heat storage. □ Measured average wall temperature at time t . △ Measured temperature at the center of the heat transfer face at time t	86
Figure 8-13: Time, t_{max} , for complete melting and temperature, T , of the heat transfer face vs. heat input rate, Q . Time for complete melting: ○ measured. ● calculated by model A. ● Calculated by models B or C. Average wall temperature at time t_{max} : □ measured. ■ calculated by model A. ■ Calculated by models B or C. △ Measured temperature at the center of the heat transfer face at t_{max}	86
Figure 8-14: Location of the thermocouples in the heat input/output face (f) and within the box (b). The thermocouples placed on the opposite face do not appear in the figure since they are projected on the same positions as those in the input/output face. All the dimensions are in mm.	89
Figure 8-15: PCM capacitors with several fillers developed by IKE. All the dimensions are in mm. a: Model 1. b: Model 2. c: Model 3. d: Model 4.	91

CEN/CLC/TR 17603-31-10:2021 (E)

- Figure 8-16: Measured temperature, T , at several points of the PCM capacitor vs. time t . Model 2. Heat up with a heat transfer rate $Q = 30,6$ W. Points are placed as follows (Figure 8-14): — Upper left corner of the heat input/output face. — Center of the insulated face. — Center of the box, immersed in the PCM. Time for complete melting t_{max} , is shown by means of a vertical trace intersecting the curves.....92
- Figure 8-17: Time for complete melting, t_{max} , vs. heat input rate Q . Model 1. ○ Measured. Model 2. □ Measured. — Calculated by using model A. Model 3. △ Measured. — Calculated by using model A. — Calculated by using model B. Model 4. ▽ Measured.92
- Figure 8-18: Largest measured temperature, T , of the heat input/output face vs. heat input rate, Q . Model 1. ○ Measured. Model 2. □ Measured. — Calculated by using model A. Model 3. △ Measured. — Calculated by using model A. — Calculated by using model B. Model 4. ▽ Measured.93
- Figure 8-19: Location of the thermocouples in the heat input/output face. The thermocouples placed on the opposite face do not appear in the figure since they are projected on the same positions as those in the input/output face. Thermocouples are numbered for later reference. All the dimensions are in mm.96
- Figure 8-20: PCM capacitor developed by IKE for ESA (ESTEC). All the dimensions are in mm. a: Box. b: Honeycomb calls. c: Perforations in compartment walls. d: Pinch tube.98
- Figure 8-21: Measured temperature, T at several points in either of the large faces of the container vs. time, t . Heat up with a heat transfer rate $Q = 86,4$ W. Points 1 to 5 are placed in the heat input/output face as indicated in Figure 8-19. Circled points are in the same positions at the insulated face. Time for complete melting, t_{max} , is shown by means of a vertical trace intersecting the curves.99
- Figure 8-22: Time for complete melting, t_{max} vs. heat input rate, Q . ○ Measured. — Calculated by using the 26 nodes model. Overall thermal conductances in the range $1,4 \text{ W.K}^{-1}$ to $5,6 \text{ W.K}^{-1}$99
- Figure 8-23: Average temperature, T of either of the large faces vs. heat input rate, Q . $t = t_{max}$. Heat input/output face. ○ Measured. — Calculated by the 26 nodes model. Overall thermal conductance $5,6 \text{ W.K}^{-1}$. — Calculated as above. Overall thermal conductance $6,7 \text{ W.K}^{-1}$. Insulated face. □ Measured. — Calculated as above. Overall thermal conductance $5,6 \text{ W.K}^{-1}$ and $6,7 \text{ W.K}^{-1}$100
- Figure 8-24: Set-up used for component tests.103
- Figure 8-25: PCM capacitor developed by B & K Engineering for NASA. All the dimensions are in mm.104
- Figure 8-26: Schematic of the PCM capacitor in the TIROS-N cryogenic heat pipe experiment package (HEPP). From Ollendorf (1976) [20].104
- Figure 8-27: Average temperature, T of the container vs. time, t , during heat up for two different heat transfer rates. ○ $Q = 25$ W. □ $Q = 45$ W. Component tests data.105
- Figure 8-28: Average temperature, T , of the container vs. time, t , during cool down. Data from either component or system tests. ○ Component tests, $Q = 6,1$ W. Freezing interval $\Delta t \approx 4,5$ h. □ System tests, $Q = 5,2$ W. Freezing

CEN/CLC/TR 17603-31-10:2021 (E)

interval $\Delta t \leq 5$ h. Time for complete melting, t_{max} , is shown by means of a vertical trace intersecting the curves.	105
Figure 8-29: Set up used for the "Beaker" tests.	108
Figure 8-30: Set up used for the "Canteen" tests.  Strain gage.  Temperature sensor.	109
Figure 8-31: PCM capacitor developed by Aerojet ElectroSystems Company. The outer diameter is given in mm.	109
Figure 8-32: "Canteen" simulation of the S day. a) Heat transfer rate, Q vs. time, t . b) PCM temperature, T , vs. time t . Data in the insert table estimated by the compiler through area integration and the value of h_f in Tables 8-9 and 8-10.	110
Figure 8-33: Maximum diurnal temperature, T of the radiator vs. orbital time, t .  Predicted with no-phase change.  Measured. Phase-change attenuated the warming trend of the radiator for eleven months (performance extension).	110
Figure 8-34: Location of the thermocouples and strain gages in the test unit. Thermocouples 12, 17 and 14 are placed on the base; 6, 7 and 8 on the upper face; 9 and 10 on the lateral faces; 11 on the rim, and 26 on the mounting hub interface. Strain gages are placed on his upper face.	114
Figure 8-35: PCM capacitor developed by Aerojet. All the dimensions are in mm.	114
Figure 8-36: Average temperature, T , of the container vs. time, t , either during heat up or during cool down. a) During heat up with a nominal heat transfer rate $Q = 2,5$ W. b) During cool down with the same nominal heat transfer rate. With honeycomb filler. Mounting hub down.  Measured.  Calculated. Cooling coils down.  Measured.  Calculated. Without honeycomb filler. Cooling coils up.  Measured.  Calculated with the original model.  Calculated with the modified model. Cooling coils down.  Measured. Times for 90% and complete melting (freezing) are shown in the figure by means of vertical traces intersecting the calculated curves. Replotted by the compiler, after Bledjian, Burden & Hanna (1979) [6], by shifting the time scale in order to unify the initial temperatures.	115
Figure 8-37: Several TRANS TEMP Containers developed by Royal Industries for transportation of temperature- sensitive products. a: 205 System. b: 301 System. c: 310 System. 1: Outer insulation. 2: PCM container.	125
Figure 8-38: Measured ambient and inner temperatures, T vs. time, t , for several TRANS TEMP Containers holding blood samples. a: 205 System. b: 301 System. c: 310 System.  Ambient temperature.  Inner temperature.	125

Tables

Table 5-1: Supercooling Tests.	17
Table 5-2: PARAFFINS	22
Table 5-3: NON-PARAFFIN ORGANICS ^a	23
Table 5-4: SALT HYDRATES	24
Table 5-5: METALLIC	26
Table 5-6: FUSED SALT EUTECTICS	27

CEN/CLC/TR 17603-31-10:2021 (E)

Table 5-7: MISCELLANEOUS	27
Table 5-8: SOLID-SOLID	28
Table 5-9: PARAFFINS	29
Table 5-10: PARAFFINS	30
Table 5-11: PARAFFINS	32
Table 5-12: NON-PARAFFIN ORGANICS	34
Table 5-13: NON-PARAFFIN ORGANICS	35
Table 5-14: NON-PARAFFIN ORGANICS	37
Table 5-15: NON-PARAFFIN ORGANICS	39
Table 5-16: NON-PARAFFIN ORGANICS	40
Table 5-17: SALT HYDRATES	42
Table 5-18: METALLIC AND MISCELLANEOUS	45
Table 6-1: Physical Properties of Several Container and Filler Materials	54
Table 6-2: Compatibility of PCM with Several Container and Filler Materials	55

European Foreword

This document (CEN/CLC/TR 17603-31-10:2021) has been prepared by Technical Committee CEN/CLC/JTC 5 “Space”, the secretariat of which is held by DIN.

It is highlighted that this technical report does not contain any requirement but only collection of data or descriptions and guidelines about how to organize and perform the work in support of EN 16603-31.

This Technical report (TR 17603-31-10:2021) originates from ECSS-E-HB-31-01 Part 10A.

Attention is drawn to the possibility that some of the elements of this document may be the subject of patent rights. CEN [and/or CENELEC] shall not be held responsible for identifying any or all such patent rights.

This document has been prepared under a mandate given to CEN by the European Commission and the European Free Trade Association.

This document has been developed to cover specifically space systems and has therefore precedence over any TR covering the same scope but with a wider domain of applicability (e.g.: aerospace).

1

Scope

Solid-liquid phase-change materials (PCM) are a favoured approach to spacecraft passive thermal control for incident orbital heat fluxes or when there are wide fluctuations in onboard equipment.

The PCM thermal control system consists of a container which is filled with a substance capable of undergoing a phase-change. When there is an the increase in surface temperature of spacecraft the PCM absorbs the excess heat by melting. If there is a temperature decrease, then the PCM can provide heat by solidifying.

Many types of PCM systems are used in spacecrafts for different types of thermal transfer control.

Characteristics and performance of phase control materials are described in this Part. Existing PCM systems are also described.

The Thermal design handbook is published in 16 Parts

TR 17603-31-01	Thermal design handbook – Part 1: View factors
TR 17603-31-02	Thermal design handbook – Part 2: Holes, Grooves and Cavities
TR 17603-31-03	Thermal design handbook – Part 3: Spacecraft Surface Temperature
TR 17603-31-04	Thermal design handbook – Part 4: Conductive Heat Transfer
TR 17603-31-05	Thermal design handbook – Part 5: Structural Materials: Metallic and Composite
TR 17603-31-06	Thermal design handbook – Part 6: Thermal Control Surfaces
TR 17603-31-07	Thermal design handbook – Part 7: Insulations
TR 17603-31-08	Thermal design handbook – Part 8: Heat Pipes
TR 17603-31-09	Thermal design handbook – Part 9: Radiators
TR 17603-31-10	Thermal design handbook – Part 10: Phase – Change Capacitors
TR 17603-31-11	Thermal design handbook – Part 11: Electrical Heating
TR 17603-31-12	Thermal design handbook – Part 12: Louvers
TR 17603-31-13	Thermal design handbook – Part 13: Fluid Loops
TR 17603-31-14	Thermal design handbook – Part 14: Cryogenic Cooling
TR 17603-31-15	Thermal design handbook – Part 15: Existing Satellites
TR 17603-31-16	Thermal design handbook – Part 16: Thermal Protection System

2 References

EN Reference	Reference in text	Title
EN 16601-00-01	ECSS-S-ST-00-01	ECSS System - Glossary of terms
TR 17603-30-06	ECSS-E-HB-31-01 Part 6	Thermal design handbook – Part 6: Thermal Control Surfaces
TR 17603-30-11	ECSS-E-HB-31-01 Part 11	Thermal design handbook – Part 11: Electrical Heating

All other references made to publications in this Part are listed, alphabetically, in the **Bibliography**.

koniec náhľadu – text ďalej pokračuje v platenej verzii STN